Supporting Information for the Manuscript "Ab Initio Confirmation of a Harpoon-Type Electron Transfer in a Helium Droplet"

María Pilar de Lara-Castells,*,† Andreas W. Hauser,*,‡ and Alexander O. Mitrushchenkov¶

Instituto de Física Fundamental, C.S.I.C., Serrano 123, E-28006 Madrid, Spain, Graz University of Technology, Institute of Experimental Physics, Petersgasse 16, 8010 Graz, Austria, and Université Paris-Est, Laboratoire Modélisation et Simulation Multi Echelle, MSME UMR 8208 CNRS, 5 bd Descartes, 77454 Marne-la-Vallée, France

E-mail: Pilar.deLara.Castells@csic.es; andreas.w.hauser@gmail.com

The first section of this Supporting Material contains information about the diabatization technique and electronic couplings obtained in the work. Section S2 presents electron transfer probabilities calculated at MS-CASPT2 level of theory. Section S3 outlines the He density functional-based approach used to calculate the repulsive contribution to the Cs_x–C_{60} ($x = 1,2$) interaction energies due to the presence of a He_{2000} droplet. It also presents two pictures showing the helium density layering around the fullerene C_{60} molecule and the calculated repulsive energy corrections. Section S4 shows how the crossing points has been estimated from experimental data. Section S5

*To whom correspondence should be addressed

†Instituto de Física Fundamental, C.S.I.C., Serrano 123, E-28006 Madrid, Spain

‡Graz University of Technology, Institute of Experimental Physics, Petersgasse 16, 8010 Graz, Austria

¶Université Paris-Est, Laboratoire Modélisation et Simulation Multi Echelle, MSME UMR 8208 CNRS, 5 bd Descartes, 77454 Marne-la-Vallée, France

presents the reaction energy pathways derived from a HF+D_{as}[CCSD(T)] ansatz. Section S6 compares test calculations on the Cs_2–C_{60} model system at CCSDT(T), MP2, and SCS-MP2 levels of theory as well as using different basis set sizes for carbon atoms. Finally, Section S7 presents interaction potentials and reaction energy pathways upon accounting for the basis set superposition error via the counterpoise scheme.

Contents

S1 Obtaining Diabatic HF Solutions and Electronic Couplings for Neutral and Ionic Channels

Strictly speaking, it is not possible to obtain HF solutions for two states of the same symmetry, as with the proper orbital optimization, the HF procedure should always end up at the electronic ground state. However, by the construction of suitable initial orbitals, biased either towards the neutral or the ionic channel, the HF algorithm can get deliberately trapped in the corresponding local minima. A similar strategy has been previously used in Ref. 1 to study the hopping between the van der Waals (vdW) and ionic electronic states characterizing the interaction of O_2 with a reduced $TiO_2(110)$ surface. This strategy has also worked for the Cs_x–C_{60} system ($x = 1, 2$). Starting from a large distance of at 100 Å between the Cs_x and C_{60} fragments, we build the initial set of orbitals by explicitly combining the orbitals associated to the HF orbitals of separated fragments using the MERGE procedure of MOLPRO.[2] At such large distances, these perfectly correspond to converged HF solutions. These orbitals are then used as starting guess to obtain solutions at smaller distance. Thus, using always the next larger distance as a starting guess, we obtain two different HF solutions corresponding to the neutral and ionic channels, which are easily monitored by calculating the dipole moment of the complete Cs_x–C_{60} system. This approach is working up to distances of about 5 Å, i.e. the location of the repulsive wall. Still, the fact that the upper HF solution is a saddle point and not the minimum, translates to a rather slow convergence of the upper state, and even non-convergence for certain distances.

It is clear that at finite distances these solutions are neither orthonormal nor non-interacting. Denoting the HF solutions obtained by MOLPRO as $\psi^0_{n,i}$, we have an overlap of the electronic wavefunctions

$$s^0_{ni} = \langle \psi^0_n | \psi^0_i \rangle \neq 0$$

and non-vanishing matrix elements for the electronic Hamiltonian

$$H^0_{ni} = \langle \psi^0_n | \hat{H} | \psi^0_i \rangle \neq 0$$

in the basis of the electronic states. To calculate these quantities, we use a specially developed procedure in MOLPRO, based on bi-orthogonal orbital transformation (see Ref. 1 for details). The present implementation works for HF wavefunctions, using the integral-direct approach, and can be applied to large systems such as molecular oxygen adsorbed to a cluster model of the $TiO_2(110)$ surface.[1]

In a first step, these HF solutions need to be orthogonalized. This is done via Schmidt orthogonalization by applying the transformation matrix

$$\begin{pmatrix} 1 & \frac{-s^0_{ni}}{\sqrt{1-s^{02}_{ni}}} \\ 0 & \frac{1}{\sqrt{1-s^{02}_{ni}}} \end{pmatrix}$$

or via the symmetric orthogonalization using the matrix

$$\begin{pmatrix} 1 & s^0_{ni} \\ s^0_{ni} & 1 \end{pmatrix}^{-1/2},$$

and transforming the energy matrix

$$\begin{pmatrix} E^0_n & H^0_{ni} \\ H^0_{ni} & E^0_i \end{pmatrix}$$

accordingly. The corresponding transformed energy matrix elements can be considered as the “diabatic" energies (diagonal elements) and “diabatic" electronic couplings (non-diagonal elements). However, the two different orthogonalization schemes (Schmidt and symmetric orthogonalization procedures) lead to a rather different non-diagonal interaction and thus they can not be considered as satisfactory.

To obtain more rigorous diabatic solutions, we have applied the method described in Ref. 3. Diabatic solutions are defined as those for which the derivative coupling is zero. Thus, it is clear that the diabatic solution is defined up to an arbitrary geometry-independent unitary transformation. In our case, it is obvious to consider that the diabatic states should coincide with the adiabatic ones

at very large distance. Then, the diabatization procedure consists in rotating the two states at the present geometry in such a way that their overlap with the diabatic states at the next larger distance is maximized. As shown in Ref. 3, this results in the following transformation matrix,

$$\hat{T}_c = \hat{S}_{cp} \left[\hat{S}_{cp}^t \hat{S}_{cp} \right]^{-1/2}$$

where $\hat{S}_{cp}$ is the overlap matrix between the HF solutions at the current geometry (orthogonalized as explained above with any orthogonalization scheme), and the diabatic solutions evaluated at a previous larger distance. Applying this transformation to the current solutions, we obtain diabatic solutions at the current geometry. Clearly, the results will not depend on the orthogonalization scheme if we start from a very large distance where the overlap s_{ni}^0 is very close to zero and thus the two orthogonalization schemes provide the same results. This diabatization method is robust even when using large steps between adjacent geometries. Still, the step should be shorter than $1-2$ Å as otherwise the S_{cp} matrix elements become very small and thus prone to numerical noise. For our system, we start from 30 Å inwards. To better estimate the crossing position between vdW and ionic states, the diabatic HF solution correlating to the C_{60}^- + Cs_x^+ fragmentation is asymptotically corrected using experimental values of the C_{60} electron affinity[4] and the Cs_x ionization energy.[5]

S2 Hopping Probabilities at MS-CASPT2 Level of Theory

As an alternative to calculate the non-adiabatic interaction between vdW and ionic states we adopted the following strategy. First, using these two HF solutions, we construct the combined one-particle density matrix as an average of the densities of the two HF solutions. Next, we generate the natural orbitals, corresponding to this averaged density. Finally, we perform the state-averaged CASSCF calculations for the two states, using a slightly increased active space to fully reproduce the corresponding HF solutions, without optimization of orbitals. This results in two adiabatic states equivalent to the original HF solutions. To recover some part of the dynamic correlation, the MS-CASPT2 method is further applied. For the Cs–C_{60} system, the valence space consists of

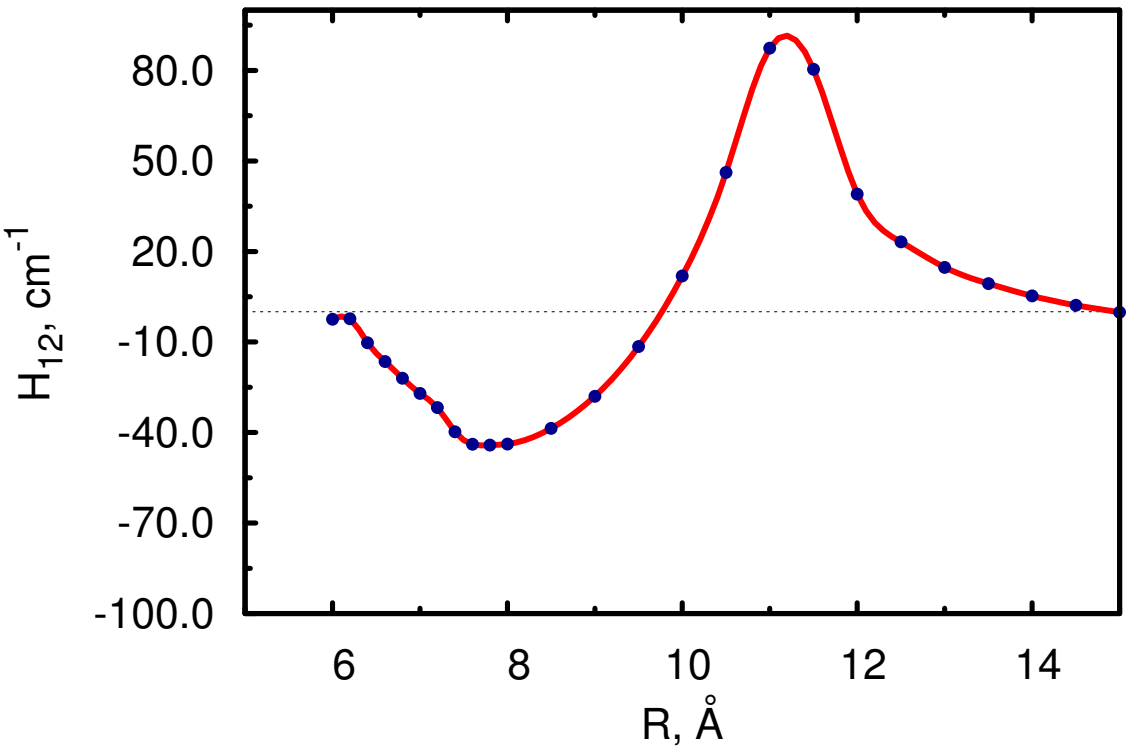

Figure S1: Electronic coupling H_{12} between vdW and ionic states as a function of the distance between Cs and C_{60} fragments.

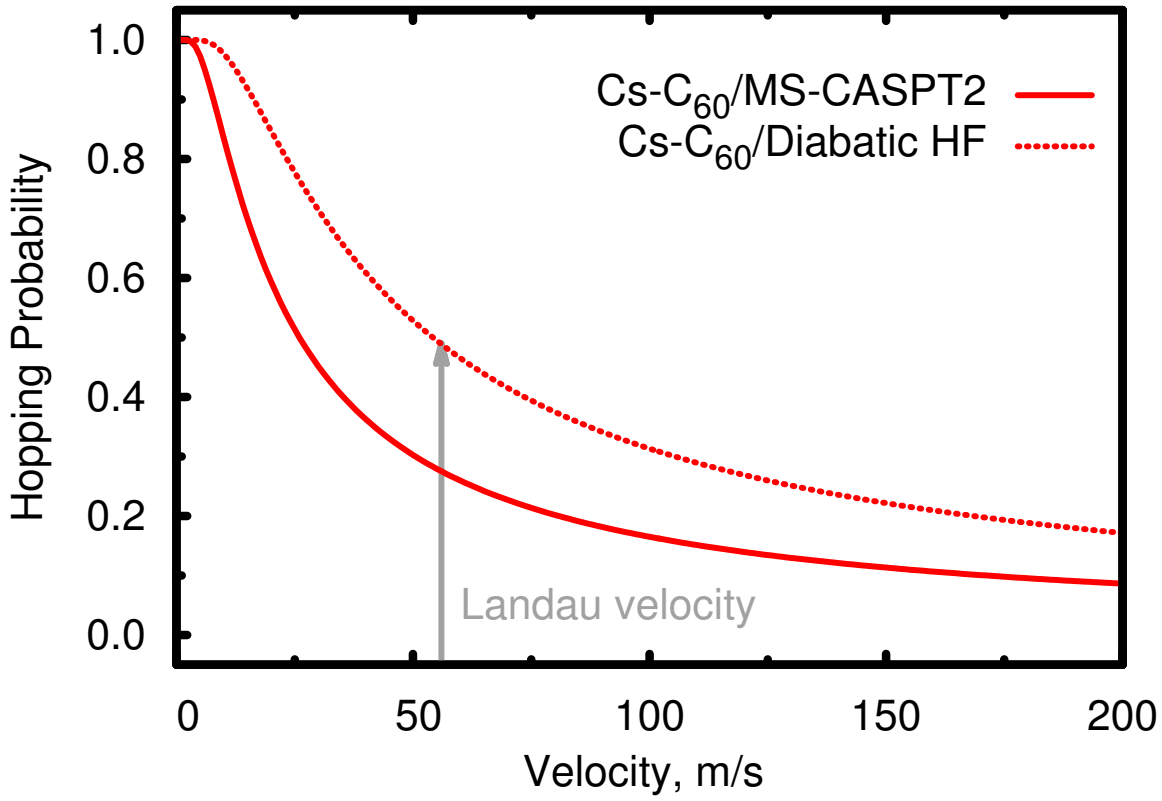

Figure S2: Hopping probabilities calculated at diabatic HF and MS-CASPT2 level of theory for the electron transfer between Cs and C_{60} fragments.

4 closed and 7 active orbitals, while inner 179 orbitals were kept frozen (not correlated). At the crossing point, half of the minimum energy splitting between these adiabatic states can be identified with the non-adiabatic interaction matrix element H_{12}. The resulting hopping probabilities as a function of the relative velocities are plotted in Figure S2. They are larger than those calculated at diabatic HF level by about 20%. If the procedure is repeated for the Cs_2–C_{60} system in a collinear configuration, the hopping probability increases to 98% at the Landau velocity, which is 27% larger than that calculated at diabatic HF level (71%). However, the value obtained for the orientational average by considering both collinear and T-shaped configurations is very similar at MS-CASPT2 and diabatic HF levels (48% vs. 52%).

S3 Calculation of the Repulsive Contribution to the Interaction Energies Between Cs_x and C_{60} Species in Helium Droplets

S3.1 Outline of Helium Density Functional Theory

Free energies of doped He nanodroplets (He_N) have been obtained via helium density functional theory (He-DFT) based on a slightly modified version of the Orsay-Trento-density functional.[6,7] The free energy of a doped He droplet is minimized with respect to a given arrangement of the dopants within the droplet and on its surface. The free energy $F[\rho]$, a functional of the helium density ρ, can be written as

$$F[\rho] = E[\rho] + U_{\text{ext}}[\rho] - \mu N[\rho] - \mathbf{F}\cdot\mathbf{R}[\rho], \tag{S1}$$

where $E[\rho]$ stands the Orsay-Trento-density functional[6] and $U_{\text{ext}}[\rho]$ an external potential introducing the interaction between the droplet and the dopants. The He–C_{60} and He–Cs_x interaction potentials reported in Ref. 8 were used. The interactions between the dopants themselves were added a posteriori (see next subsection). The two last terms of the equation allows for the conservation of N, the total particle number, and $\mathbf{R}$, the He droplet mass center. Both can be written as

functionals of the density,

$$N = \int d\mathbf{r}\,\rho(\mathbf{r}) \;\;,\;\; \mathbf{R} = \frac{1}{N}\int d\mathbf{r}\,\rho(\mathbf{r})\mathbf{r}. \tag{S2}$$

Their corresponding Lagrange parameters are the chemical potential μ and the retaining force $\mathbf{F}$, respectively. The density functional itself can be written as[7]

$$\begin{aligned} E[\rho] &= \frac{\hbar^2}{2m}\int d\mathbf{r}(\nabla\sqrt{\rho}) \\ &+ \frac{1}{2}\int d\mathbf{r}\,d\mathbf{r}'\,V_{\mathrm{LJ}}(|\mathbf{r}-\mathbf{r}'|)\rho(r)\rho(r') \\ &+ \frac{c_2}{2}\int d\mathbf{r}\rho(\mathbf{r})\bar{\rho}(\mathbf{r})^2 + \frac{c_3}{2}\int d\mathbf{r}\rho(\mathbf{r})\bar{\rho}(\mathbf{r})^3 \\ &+ C\int d\mathbf{r}\,\left[1+\tanh\left(\beta\{\rho(\mathbf{r})-\rho_m\}\right)\right], \end{aligned} \tag{S3}$$

with the first term as the quantum kinetic energy, the second as a Lennard-Jones-type He-He pair potential interaction energy, term 3 and 4 as short range correlation energy contributions involving $\bar{\rho}$, a locally averaged density for a given sphere of radius $\bar{h}$, and finally, a penalty term which forbids unphysical pile-up of He density.[7]

S3.2 Calculation of the Repulsive Energy Correction due to the Presence of a He_{2000} Droplet

The aim of this subsection is to briefly outline how we have calculated the repulsive energy contribution to the interaction of Cs or Cs_2 with C_{60} in the environment of superfluid helium at a temperature of 0.38 K. We simulate the experimental conditions,[9] where a sequential pickup of C_{60} fullerenes and Cs atoms was studied by electron ionization mass spectrometry. While heliophilic fullerenes immerse into the droplet completely, the heliophilic alkali metals are known to reside on the droplet surface due to their diffuse valence electron density. This spatial separation, which occurs in cases where C_{60} pickup takes place before Cs pickup, together with the hindered

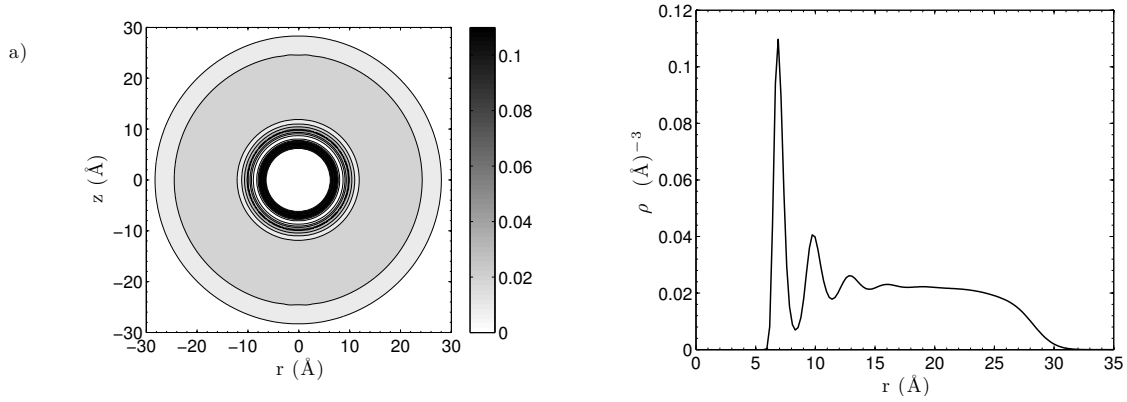

Figure S3: Left-hand panel: contour plot of the helium density for the He_{2000} droplet with the C_{60} molecule immersed (at its center). Right-hand panel: average helium density at a function of the radial distance to the center of the drop where the C_{60} molecule is located. The density is plotted in units of $Å^{-3}$. Note that the bulk value for the density of liquid helium is 0.02185 per $Å^{-3}$.

mobility of the dopants on and in the droplet,[10] introduces a repulsive energy correction to the interaction between the dopants.

One example density distribution for the C_{60} fullerene immersed in the He droplet consisting of $N = 2000$ He atoms is shown in Figure S3 as a contour plot of planar cut through the system (left-hand panel), and as the average over the radial distance to the drop center (right-hand panel). Note the helium shell of exceptionally high density which surrounds the fullerene. Next, the total energy of the multiply-doped He_{2000} droplet is evaluated via He-DFT as a function of the distance between the heliophilic and the heliophobic dopant. By repeating the He-DFT energy evaluations for intermolecular distances from 5 to 40 Å we obtain the energy corrections shown in Figure S4, which have been added to the interaction between the dopants (see Figures 1 and 3 of the main manuscript).

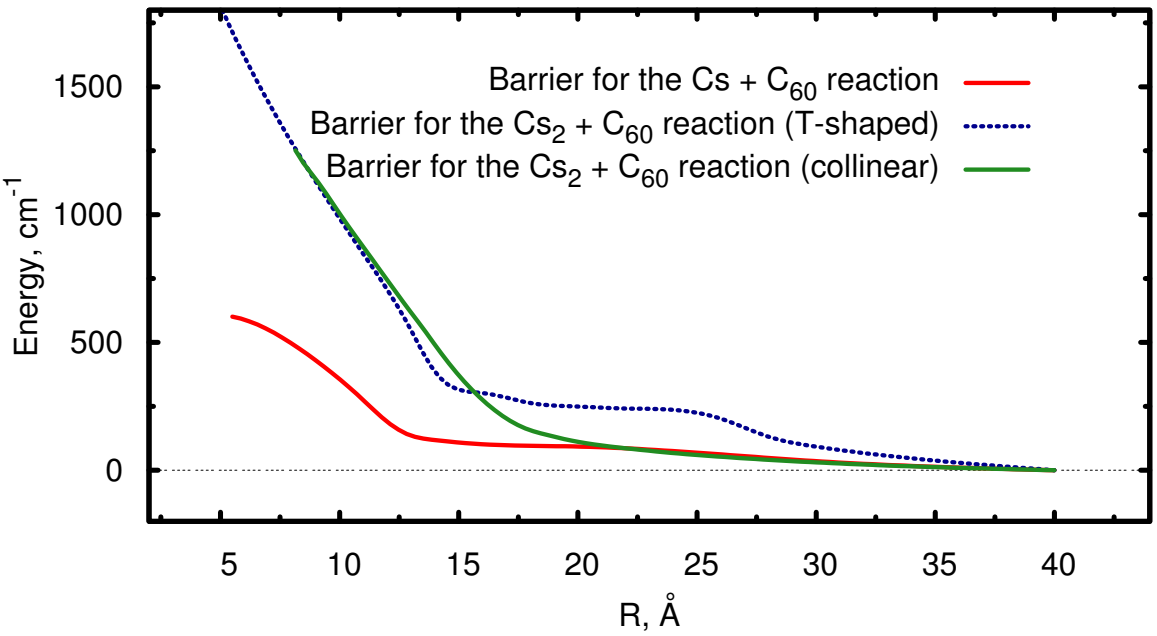

Figure S4: Repulsive corrections which occur due to sterical hindrance during the reaction of Cs or Cs_2 with C_{60} inside a helium droplet formed by 2000 He atoms, evaluated with orbital-free helium density functional theory.

S4 Determination of Crossing Points from Experimental Data

The position of the crossing point R_x can be estimated by assuming a $-1/R$ asymptotic behaviour of the ionic potential energy curve and solving the following equation,

$$-1/R_x + \Delta E = 0 \tag{S4}$$

with $\Delta E = \mathrm{IE} - \mathrm{EA}$, where IE is the ionization energy of the Cs_x fragment and EA is the electron affinity of the C_{60} molecule. Experimental values have been used for both IE and EA values of atomic cesium[5] and the C_{60} molecule.[4] The resulting ΔE value is 9840 cm^{-1} for the Cs–C_{60} system, with R_x being 11.8 Å. The ΔE value for the $Cs_2(a\ ^3\Sigma_u^+)$–C_{60} complex is estimated to be 5535 cm^{-1} instead, with R_x being 21.4 Å. To derive this value, we use the experimental-based data for both the vdW well-depth and position of the potential minimum of the $Cs_2(a\ ^3\Sigma_u^+)$ dimer

(295 cm^{-1} and 6.3 Å from Ref. 11) as well as the interaction energy of the Cs_2^+ molecule at 6.3 Å (about 4700 cm^{-1}).

S5 Reaction Energy Pathways Derived from a HF + D_{as}[CCSD(T)] Ansatz

Another approach to add the dispersion contribution to the diabatic HF solution in the neutral state is based on an extrapolation of the correlation contributions calculated for vdW Cs_x-benzene complexes at single and double and perturbative triples coupled cluster [CCSD(T)] level in our previous work.[8] These interaction energies were counterpoise-corrected.[12] As mentioned in Ref. 8, CCSD(T) calculations are first performed for the vdW Cs_x–benzene complexes. The correlation CCSD(T) energies are then fitted to the effective interatomic pairwise D_{as} function proposed by Szalewicz and collaborators.[13,14] Finally, the function D_{as} is used to estimate the dispersion contribution to the interaction energies of the vdW Cs_x–C_{60} complexes, adding them to those obtained at diabatic HF level.

As can be seen in Figure S5, the global picture emerging from the calculated reaction energy path is very similar to that obtained using the MP2 method (see Figure 3 of the main manuscript): The energetic barrier emerging from the extrusion of helium upon the approach of the two reactants at the crossing region is overcome for the Cs_2–C_{60} system in a collinear approach at the Landau velocity, but neither by atomic cesium nor the Cs_2–C_{60} complex at a T-shaped configuration.

S6 Test Calculations on the Cs_2-Benzene Model System

Test calculations have been performed for the Cs_2–C_{60} model system at CCSD(T), MP2, and spin-component scaled[15] (SCS-MP2) levels of theory, with the Cs_2 in the ground (singlet) state at a collinear approach with the C_6 axis of benzene. The CCSD(T) calculations were perfomed using the polarized correlation-consistent double-ζ basis set for carbon atoms (as for the Cs_x–C_{60}

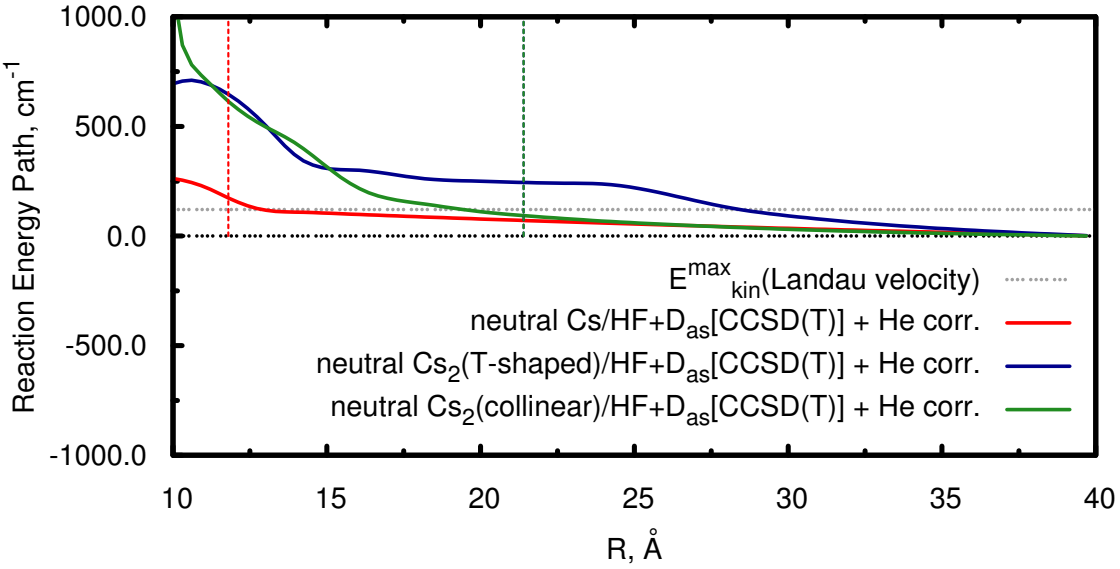

Figure S5: Reaction energy paths as calculated at HF+D_{as}[CCSD(T)] level. Dashed lines indicate the positions of the crossing points, as determined from experimental estimations (see section S4).

system) as well as the augmented polarized correlation-consistent triple-ζ counterpart.[16] These basis sets will be referred to as cc-pVDZ and aug-cc-pVTZ.

As can be seen in Figure S6, the MP2 method overestimates the well-depth by about 19% as compared with the CCSD(T) treatment when using the same basis set. It can be also observed that the separate scaling of the parallel and anti-parallel spin components proposed by Grimme[15] corrects the MP2 overbinding. However, we notice that the MP2 overestimation of the binding energy is partially compensated by the incompleteness of the basis set centered at the carbon atoms: the MP2 interaction energies obtained using the cc-pVDZ basis are very similar to the CCSD(T) counterparts calculated with the aug-cc-pVTZ basis.

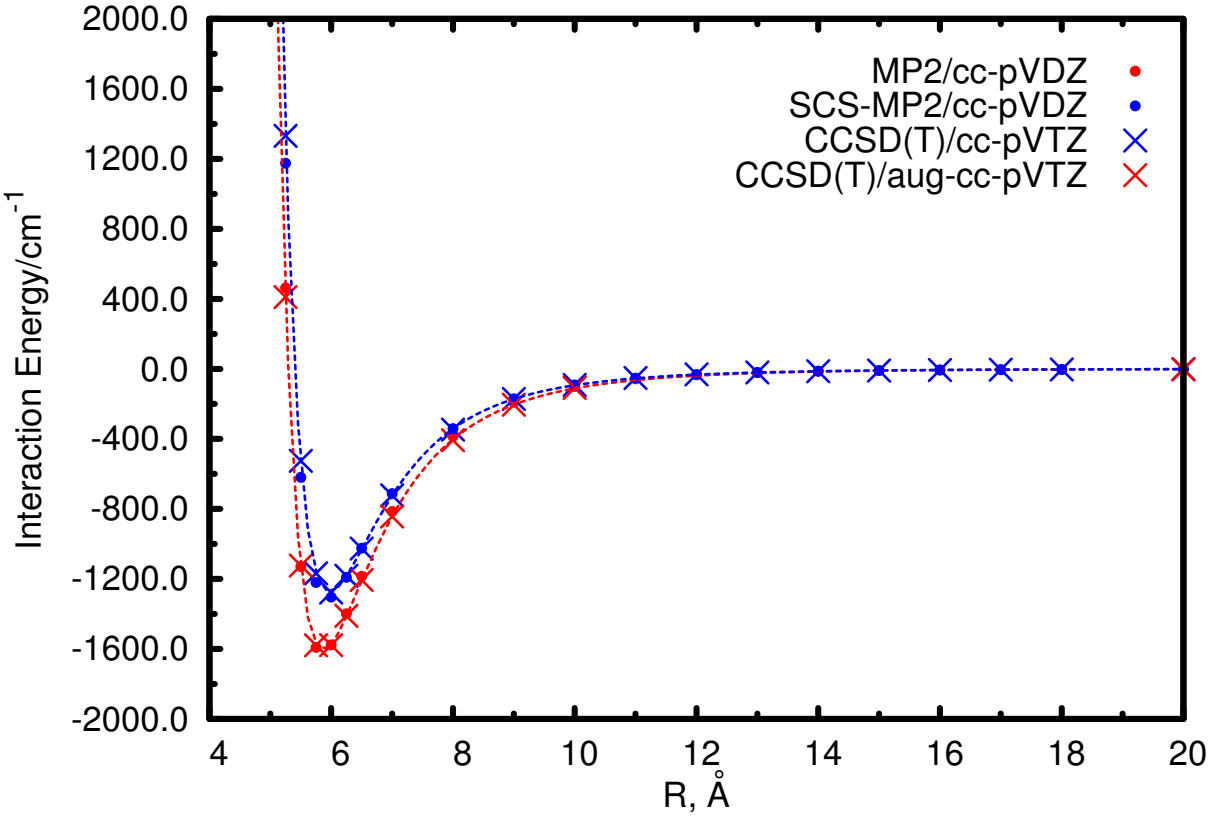

Figure S6: Cs_2-benzene interaction energies as a function of the distance from the Cs_2 to the benzene center-of-mass positions. The Cs_2 intramolecular axis is collinear to the C_6 symmetry axis of the benzene molecule. The interaction energies have been obtained in the adiabatic representation, asymptotically correlated to a separation in neutral fragments. The potential minimum corresponds to the interaction between a negatively charged benzene molecule and a positively charged Cs_2 species.

S7 Counterpoise-Corrected Interaction Energies and Reaction Energy Pathways

To get insights into the influence of the basis set superposition error (BSSE), we have applied the counterpoise correction scheme of Boys and Bernardi[12] to the MP2 interaction energies associated to both neutral and ionic states of the Cs_2–C_{60} system. We considered the particular case where the Cs_2 intramolecular axis is collinear to the C_3 symmetry axis of the C_{60} molecule. For the neutral state, counterpoise-corrected energies $E^{\mathrm{CP}}_{\mathrm{Cs_2-C_{60}}}$ were calculated as a function of the distance between the Cs_2 to the C_{60} center-of-mass positions R as,

$$E^{\mathrm{CP}}_{\mathrm{Cs_2-C_{60}}}(R) = E_{\mathrm{Cs_2-C_{60}}}(\infty) + E_{\mathrm{Cs_2-C_{60}}}(R) - E_{\mathrm{Cs_2}}(R) - E_{\mathrm{C_{60}}}(R) \tag{S5}$$

where $E_{\mathrm{Cs_2-C_{60}}}$ is the MP2 energy of the Cs_2–C_{60} dimer in the neutral state, and $E_{\mathrm{Cs_2}}$ and $E_{\mathrm{C_{60}}}$ are the MP2 energies of the neutral (ground-state) interacting monomers, as calculated with the dimer basis set at the geometry of the dimer.

For the ionic state, counterpoise-corrected energies $E^{\mathrm{CP}}_{\mathrm{Cs_2^+-C_{60}^-}}$ are estimated in a similar way as

$$E^{\mathrm{CP}}_{\mathrm{Cs_2^+-C_{60}^-}}(R) = E_{\mathrm{Cs_2^+-C_{60}^-}}(\infty) + E_{\mathrm{Cs_2^+-C_{60}^-}}(R) - E_{\mathrm{Cs_2^+}}(R) - E_{\mathrm{C_{60}^-}}(R) \tag{S6}$$

where $E_{\mathrm{Cs_2^+-C_{60}^-}}$ is the MP2 energy of the $\mathrm{Cs_2^+ - C_{60}^-}$ ionic dimer, and $E_{\mathrm{Cs_2^+}}$ and $E_{\mathrm{C_{60}^-}}$ are the MP2 energies of the ionic interacting monomers, as calculated with the dimer basis set at the geometry of the dimer. To estimate the energy of the ionic state at dissociation, we used the distance of $R = 100$ Åadding the pure Coulomb term $1/R$. The electronic clouds of ionic states are interacting via the long range Coulomb and higher electrostatic terms which makes it more difficult to define the BSSE correction. To verify the quality of the long-range interaction, we compared the total energy of the complex and the sum of monomer energies together with the Coulomb $1/R$ interaction, the difference being below 2 $\mathrm{cm^{-1}}$ at 100 Å. As the ionic character of the diabatic states is well preserved, we think that the above approach provides reasonable estimate of BSSE effects for both

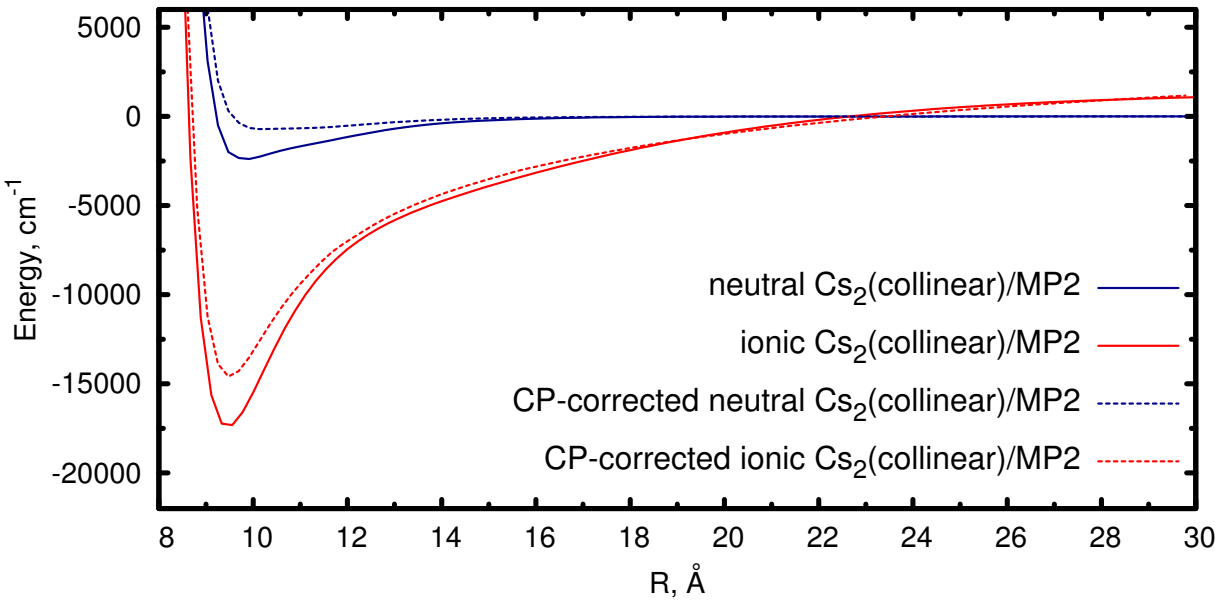

Figure S7: Cs_2–C_{60} interaction energies in neutral and ionic states using the MP2 method, as a function of the distance between the Cs_2 to the C_{60} center-of-mass positions. The Cs_2 intramolecular axis is collinear to the C_3 symmetry axis of the C_{60} molecule. Counterpoise corrected[12] interaction energies are presented and compared with those excluding this correction.

neutral and ionic states.

In Figure S7, we compare the interaction energies obtained with and without including the counterpoise correction for both neutral and ionic states. As expected, the potential minima regions are shallower upon including the counterpoise correction. Thus, the value of the well-depth for the ionic state is 2850 cm^{-1} smaller (about 16% of the interaction). The influence on the energy at the potential minimum for the van der Waals-dominated interaction in the neutral state is much more pronounced: the shaft region is about three times less deeper. However, it is very important to stress that the crossing region is almost unperturbed by this correction. This is clearly seen in Figure S8, showing the solvation-corrected reaction paths, i.e. the interaction energies corrected by the repulsion energy contribution arising from the He extrusion upon the approach of the Cs_2 and C_{60} reactive species. It can be observed that the solvation-corrected reaction paths with and without including the counterpoise correction are almost coinciding. Also, it is worth stressing that the energetic barrier to the vdW potential minimum becomes more pronounced upon incorporating

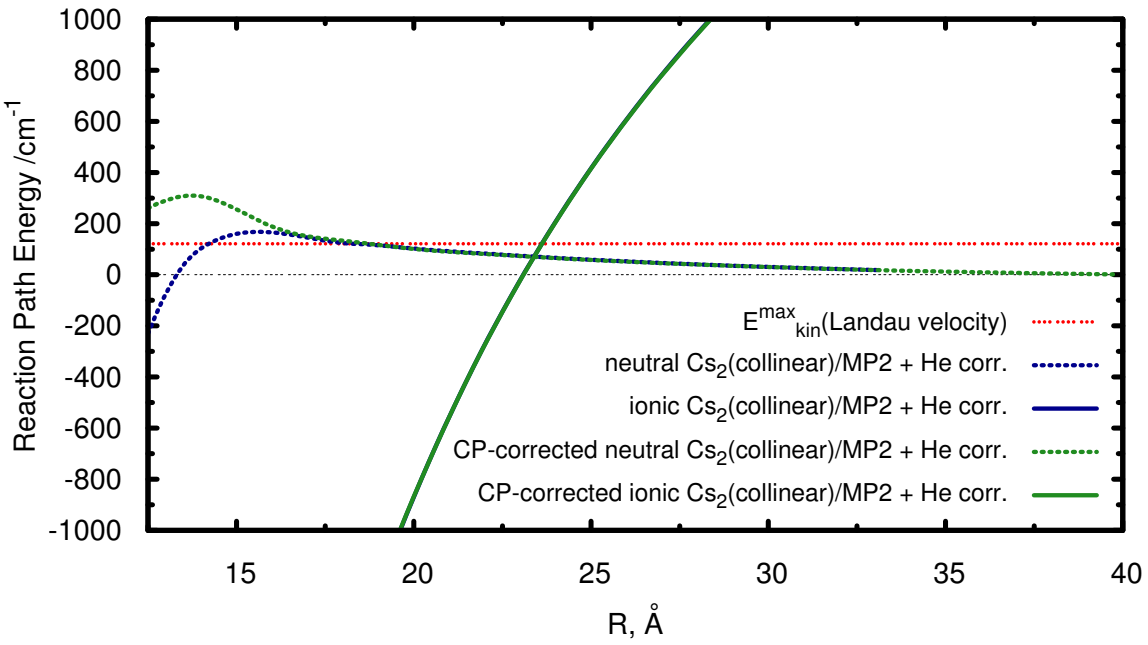

Figure S8: Solvation-corrected reaction paths in the diabatic representation for the formation of either the vdW Cs_2–C_{60} or ionic Cs_2^+–C_{60}^- complexes at MP2 level, with and without including the counterpoise correction[12] as an estimate of the basis set superposition error (BSSE).

the counterpoise correction, thus reinforcing our conclusions about the destabilization of the vdW complex.

Similar effects can be expected in counterpoise-corrected reaction energy paths for the T-shaped configuration of the reactive Cs_2 and C_{60} species. On one hand, the crossing point (at 22.3 Å) is too far away from the potential minimum for the counterpoise correction to have an influence. On the other hand, the energetic barrier to the vdW potential minimum is expected to become even larger than without including the counterpoise correction. We also notice that the crossing between neutral and ionic states occurs at a shorter relative distance for the Cs–C_{60} system (about 12.1 Å) so that the counterpoise correction has an influence by making the energy barrier to the ionic state even larger (to about 200 cm^{-1}), as well as that to the vdW potential minimum (to about 300 cm^{-1}), thus reinforcing the main conclusions of this work.

References

(1) de Lara-Castells, M. P.; Mitrushchenkov, A. O.; Roncero, O.; Krause, J. L. Adsorption and Nonadiabatic Processes in the Photodesorption of Molecular Oxygen from the Reduced TiO_2(110) Surface. *Isr. J. Chem.* **2005**, *45*, 59–76.

(2) Werner, H. J.; Knowles, P. J.; Knizia, G.; Manby, F. R.; Schütz, M.; Celani, P.; Korona, T.; Lindh, R.; Mitrushchenkov, A. O.; Rauhut, G.; et al., MOLPRO, version 2012.1, a package of *ab initio* programs, see http://www.molpro.net.

(3) Mitrushenkov, A. O.; Palmieri, P.; Puzzarini, C.; Tarroni, R. Numerical Techniques for the Evaluation of Non-Adiabatic Interactions and the Generation of Quasi-Diabatic Potential Energy Surfaces Using Configuration Interaction Methods. *Mol. Phys.* **2000**, *98*, 1677–1690.

(4) Huang, D.-L.; Dau, P. D.; Liu, H.-T.; Wang, L.-S. High-Resolution Photoelectron Imaging of Cold C_{60} Anions and Accurate Determination of the Electron Affinity of C_{60}. *J. Chem. Phys.* **2014**, *140*, 224315.

(5) Deiglmayr, J.; Herburger, H.; Saßmannshausen, H.; Jansen, P.; Schmutz, H.; Merkt, F. Precision Measurement of the Ionization Energy of Cs I. *Phys. Rev. A* **2016**, *93*, 013424.

(6) Dalfovo, F.; Lastri, A.; Pricaupenko, L.; Stringari, S.; Treiner, J. Structural and Dynamical Properties of Superfluid Helium: A Density-Functional Approach. *Phys. Rev. B* **1995**, *52*, 1193.

(7) Ancilotto, F.; Barranco, M.; Caupin, F.; Mayol, R.; Pi, M. Freezing of ^{4}He and its Liquid-Solid Interface from Density Functional Theory. *Phys. Rev. B* **2005**, *72*, 214522.

(8) Hauser, A. W.; de Lara-Castells, M. P. Spatial Quenching of a Molecular Charge-Transfer Process in a Quantum Fluid: The Cs_x-C_{60} Reaction in Superfluid Helium Nanodroplets. *Phys. Chem. Chem. Phys.* **2017**, *19*, 1342–1351.

(9) Renzler, M.; Daxner, M.; Kranabetter, L.; Hauser, A. W.; Ernst, W. E.; Lindinger, A.; Zillich, R.; Scheier, P.; Ellis, A. M. Communication: Dopant-Induced Solvation of Alkalis in Liquid Helium Nanodroplets. *J. Chem. Phys.* **2016**, *145*, 181101.

(10) Hauser, A. W.; Volk, A.; Thaler, P.; Ernst, W. E. Atomic Collisions in Suprafluid Helium-Nanodroplets: Timescales for Metal-Cluster Formation Derived from He-Density Functional Theory. *Phys. Chem. Chem. Phys.* **2015**, *17*, 10805–10812.

(11) Li, D.; Xie, F.; Li, L.; Magnier, S.; Sovkov, V.; Ivanov, V. The 3 $^3\Sigma_g^+$ and a $^3\Sigma_u^+$ states of Cs_2: Observation and Calculation. *Chem. Phys. Lett.* **2007**, *441*, 39 – 42.

(12) Boys, S.; Bernardi, F. The Calculation of Small Molecular Interactions by the Differences of Separate Total Energies. Some Procedures with Reduced Errors. *Molecular Physics* **1970**, *19*, 553–566.

(13) Pernal, K.; Podeszwa, R.; Patkowski, K.; Szalewicz, K. Dispersionless Density Functional Theory. *Phys. Rev. Lett.* **2009**, *103*, 263201.

(14) Podeszwa, R.; Pernal, K.; Patkowski, K.; Szalewicz, K. Extension of the Hartree-Fock Plus Dispersion Method by First-Order Correlation Effects. *J. Phys. Chem. Lett.* **2010**, *1*, 550–555.

(15) Grimme, S. Improved Second-Order Möller-Plesset Perturbation Theory by Separate Scaling of Parallel and Antiparallel-Spin Pair Correlation Energies. *J. Chem. Phys.* **2003**, *118*, 9095–9102.

(16) Woon, D. E.; Dunning, T. H. Gaussian Basis Sets for Use in Correlated Molecular Calculations. IV. Calculation of Static Electrical Response Properties. *J. Chem. Phys.* **1994**, *100*.